

High-Temporal Resolution Observations of Tornadogenesis and Tornado Decay Using the Atmospheric Imaging Radar

Casey B. Griffin^{1,2}, David J. Bodine¹, Andrew Mahre^{1,2}, James M. Kurdzo^{1,2}, Javier Lujan¹, and Robert D. Palmer^{1,2}

¹Advanced Radar Research Center, University of Oklahoma, Norman, OK, U.S.A.

²School of Meteorology, University of Oklahoma, Norman, OK, U.S.A.

Background

Rapid-scan radars are uniquely qualified to interrogate the vertical evolution of rotation during tornadogenesis (Houser et al. 2013; French et al. 2013) and tornado decay (French et al. 2014). Houser et al. (2015) found that subtropical rotation in the 24 May 2011 El Reno, Oklahoma tornado first developed below 1 km and then intensification occurred simultaneously throughout the column when rotation increased aloft (e.g., above 3 km). French et al. (2014) found that the 5 June 2009 Goshen County, Wyoming, tornado first dissipated near a height of 1.5 km and then proceeded to decay in an "inside out" manner at progressively higher and lower elevations. The level where dissipation first occurred was found to be just above where the tornado motion was most influenced by outflow. Houser et al. (2015) also noted a similar decay mechanism in the El Reno tornado with tornado dissipation first occurring in a stable layer between 1.5 and 3 km above the ground. This study documents one case of tornadogenesis and one case of tornado decay using the Atmospheric Imaging Radar (AIR). The nearly simultaneous volumetric data collection by the AIR provides a unique opportunity to interrogate vertical structure without having to account for translation or evolution of the tornado between elevation scans.

23 May 2016 Woodward, Oklahoma Tornadogenesis

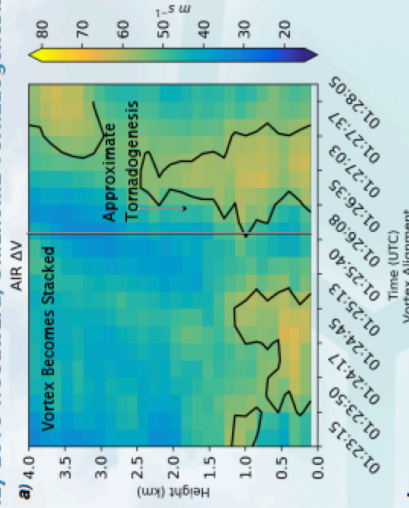


Figure 1. (a) Time-height plot of maximum ΔV ($m s^{-1}$) and (b) the distance between the mean position of the Woodward tornado in the lowest 1 km and the mean position of the vortex between 1-2 km (blue), 2-3 km (orange), and 3-4 km (green).

23 May 2016 Woodward, Oklahoma

- The intensification of rotation during tornadogenesis occurred approximately simultaneously in the vertical in the lowest 2.5 km (Figure 1a)
- Prior to reported tornadogenesis, a 2 minute period of strong rotation ($\Delta V > 60 m s^{-1}$) was observed in the lowest 1 km ARL
- At 0125 UTC, the low-level vortex weakened before intensifying back above 60 $m s^{-1}$ 90 s later, at the time when the tornado was first reported
- At 1 km ARL, values of ΔV greater than 50 $m s^{-1}$ persisted during the time when the vortex below 1 km weakened
- At 0126 UTC, just prior to tornadogenesis, the vortex became vertically stacked with the horizontal distance between the mean vortex location in the lowest 1 km and the mean vortex locations between 1-2 km, 2-3 km, and 3-4 km all decreasing to less than 200 m (Figure 1b)
- The stacked nature of the vortex was short lived, which may have contributed to the brief nature of strong ΔV
- The Woodward tornado went through at least two additional intensification periods (not shown), which will be the subject of future work

27 May 2015 Canadian, Texas Tornado Decay

- Following an initial weakening of the tornado at the beginning of the dataset, a brief, bottom-up intensification of the tornado occurred in the lowest 1 km ARL (Figure 2a)
- The intensification coincided with a narrowing of the vortex diameter within the same layer (Figure 2b)
- Vortex decay occurred in multiple modes. Decay occurred simultaneously above 1250 m, downward between 400 and 1250 m, nearly simultaneously between 150 and 400 m, and decay in the lowest 150 m slightly preceded decay between 150 and 400 m
- Decay above 1250 m was accompanied by a broadening of the vortex and the downward dissipation between 400 and 1250 m was associated with a downward increase of the radius of maximum winds

Figure 2. Time-height plots of (a) maximum ΔV ($m s^{-1}$) and (b) the distance (km) separating maximum inbound and maximum outbound velocities used to calculate ΔV in (a). Vortex diameter is thresholded on ΔV beneath 40 $m s^{-1}$.

Canadian Tornado Tilt

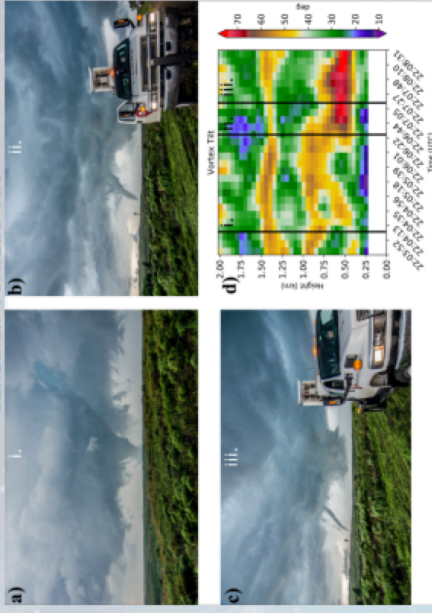


Figure 3. Photographs at (a) 2204, (b) 2206, and (c) 2207 UTC and (d) a time-height plot of filtered vortex tilt (deg). Vertical lines i, ii, iii in (d) correspond with (a-c) respectively. Photographs adapted from Kurtz et al. (2017).

- The Canadian tornado became increasingly tilted between 500-1000 m ARL late in its lifecycle (Figure 3) as the low levels of the tornado became displaced to the west of the vortex above 1 km
- A persistent region of enhanced tilted was located between 1.25 and 1.5 km ARL. This layer approximately corresponded with the level of free convection (not shown) and separated the simultaneous and downward decay modes in Figure 2a

Future Work

- Extend the Woodward analysis to include data collected before and after the shown period, which includes at least 2 additional intensification periods
- Similar analyses will be performed on tornadogenesis failure cases to determine if any differences exist in mesocyclone behavior between failure and genesis cases

References

French, M., H. Bluestein, I. PopStefanija, C. Baldi, and R. Bluth, 2013: Reexamining the vertical development of tornadic vortex signatures in supercells. *Monthly Weather Review*, **141**, 4576-4601.

French, M., H. Bluestein, I. PopStefanija, C. Baldi, and R. Bluth, 2014: Mobile, phased-array, Doppler radar observations of tornadoes at X band. *Monthly Weather Review*, **142**, 1010-1036.

Houser, J. H., Bluestein, and J. Snyder, 2015: Rapid-Scan, polarimetric, Doppler radar observations of tornadogenesis and tornado dissipation in a tornadic supercell: The "El Reno, Oklahoma" storm of 24 May 2011. *Monthly Weather Review*, **143**, 2685-2710.

Kurtz, J., F. Nai, D. Bodine, T. Bonin, R. Palmer, B. L. Cheong, J. Lujan, A. Mahre, and A. Byrd, 2017: Observations of severe local storms and tornadoes with the Atmospheric Imaging Radar. *Bulletin of the American Meteorological Society*, **57**, 527-544.

Contact the Author

If you have any questions regarding this work, please contact the author via email at casey.griffin@ou.edu



This work is partially supported by National Science Foundation grant AGS-1823478. Any opinions, findings, conclusions, or recommendations expressed in this material are those of the authors and do not necessarily reflect those of the National Science Foundation. Additional thanks must be extended to the ARCC engineering staff for maintaining the AIR.

